# Investigation of the low-temperature mechanical behaviour of elastomers and their carbon nanotube composites using microindentation

# Investigation of the low-temperature mechanical behaviour of elastomers and their carbon nanotube composites using microindentation

L.S. Fomenko[1] S.V. Lubenets[1], V.D. Natsik[1,2] , A.I. Prokhvatilov[1], N.N. Galtsov[1], Q.Q. Li[3], V. Koutsos[4]

[1]*B.I. Verkin Institute for Low Temperature Physics and Engineering, NAS of Ukraine, Kharkiv, Ukraine*
[2]*V.N. Karazin Kharkiv National University, 4 Svoboda Sq., Kharkiv, Ukraine*
[3]*Department of Aeronautics, Imperial College London, South Kensington Campus, London SW7 2AZ, United Kingdom*
[4]*School of Engineering, Institute for Materials and Processes, The University of Edinburgh, King's Buildings, Robert Stevenson Road, Edinburgh, EH9 3FB, United Kingdom*

E-mail: lubenets@ilt.kharkov.ua

Abstract

The micromechanical properties of epoxy resin elastomers and their carbon nanotube composites were studied using a microhardness tester equipped with low-temperature chamber. X-ray diffraction analysis indicated that all specimens were free of any crystalline components and were amorphous with only short-range order domains. The Vickers microhardness of all samples has been estimated in the temperature range 230-300 K. The measurements demonstrated that at room temperature these materials are elastomers (notably, they are in high-elastic state) and on cooling in the range of 250-270 K the glass transition takes place. Analysis of the temperature dependence of microhardness suggested that the thermomechanical and relaxation properties of the materials studied are consistent with a rheological model of a standard linear solid where the relaxation time (or viscosity) depends exponentially on the temperature in accordance with the Arrhenius equation for the rate of thermally activated process. Empirical estimates for the nonrelaxed and relaxed Young's moduli and also for the activation energy ($U$ = 0.75 eV) and the period of attempts ($\tau_0 = 10^{-12}$ s) of the molecular process which determines the relaxation properties and the glass transition of the materials have been obtained. The addition of carbon nanotubes into elastomeric epoxy resin had no effect on its micromechanical characteristics as measured by the microhardness tester. It is shown that the conventional microindentation method is an efficient tool of investigating the thermomechanical properties of elastomers nearby and below the glass transition temperature.

Keywords: amorphous elastomers and their carbon nanocomposites, microindentation, low-temperature microhardness, relaxation properties, glass transition

## 1. Introduction

Carbon nanotubes possessing unique geometric and mechanical characteristics [1-3] are attractive candidates for developing new high-performance nanocomposite structures of specific physico-mechanical properties. Metal-carbon composites and organic epoxy resin containing small concentrations of nanotubes [4-8] have been synthesized, which can be applicable in machine building industry and in air and space engineering.

The fabrication, microstructure and macroscopic mechanical properties of epoxy resin-carbon nanotubes composites (ER-CNT) have already been described [4-8]. The improvements in their mechanical properties depend significantly on the parameters affecting their microstructure; first of all the nanotube dispersion, the type and concentration of CNT, and on the details of the

preparation procedure of the final product which can affect the microstructure (for comprehensive information see in [4-8]). Mechanical testing at room temperature showed that the Young's modulus and strength of these composites using either hard or elastomeric epoxy were about 30-100 % higher than for the pure epoxy resin [4-8].

In physical materials science, besides the macromechanical testing of materials the task of which is in the determination of elastic moduli, yield stresses, ultimate strengths, and so on, much attention is being given to the study of the mechanical properties in nano- and microindentation experiments. The nano- and microindentation methods have been realized so far only at room and elevated temperatures. Therefore, it is not straightforward to be used for the study of elastomers which have a low-temperature glass transition. Several physical techniques allow the study of the conformation dynamics, i.e. the thermally activated motion of the nanometer-scale segments of macromolecules, which determines the mechanisms of viscoelastic deformation at the high elastic state, as well as at the glass state; these include relaxation spectrometry methods [9,10], the thermomechanical measurements [9,10], probing the temperature-frequency dependence of dynamic elastic modulus and internal friction [10], DMA [5,11], measurement of dielectric losses [12]. One of the goals of this study was to investigate the efficiency of the conventional microindentation method in studying of the rheological properties of elastomeric materials (both pure and reinforced) with the glass transition below the room temperature. The main purpose of this work laid in measuring the microhardness of pure epoxy (ER) and several specific carbon nanotube composites pairs (ER-CNT) at the low temperature range, including the glass transition regime, studying their indentation creep and analyzing the experimental data on the basis of the existing theory for the first time.

## 2. Materials and experimental technique

The samples were (crosslinked) elastomeric epoxy resin and nanocomposites based on it incorporating single- or multiwall carbon nanotubes (0.03 wt%) (see Tables 1,2). The preparation technique of the samples has been described in detail in [7, 8]. Notice that the term pure epoxy

resin (ER) as a base polymer for preparation of composites is meant as a composition of epoxy resin with hardener subjected to an appropriate heat treatment to create a crosslinked sample [7, 8]. To improve the dispersion of the nanotubes and their binding to the matrix, a block copolymer (0.3 wt %) was added to composites in some cases (Tables 1, 2).

The structure of composites was investigated by optical microscopy and the method of small-angle X-ray scattering using the polycrystalline diffractometer DRON-3M with Cu anode radiation. Using the special method of primary beam collimation and shielding, we were able to analyze diffraction patterns that were obtained in the angle interval $2\theta$ = (1.5-40) deg.

The Vickers microhardness was measured in the temperature interval 230-300 K with a standard unit PMT-3 equipped with a chamber for cooling the samples below the room temperature. To lower the temperature, the chamber with a sample was blown through with nitrogen vapor. The objective of the microscope was shielded with a thin glass coverslip. The indentation load $P$ and the loading duration $t$ were varied within $P$ = 0.005-0.40 N and $\Delta t$ = 1-150 s, respectively. The microhardness was calculated according to

$$H_V = \frac{1.854\,P}{d^2}, \tag{1}$$

where $d$ is the length of the residual impression diagonal.

The composites investigated at room temperature exhibited a high-elasticity, which is inherent of some class of polymers [9]. In indentation experiments the loading-produced impression on the sample surface disappeared completely when the indenter was lifted. Hence, for the measurements of microhardness at room temperature, we used the technique of deposition of metallic Al and In films onto the sample surface or coating the surface of the indenter pyramid with Ramsay lubrication grease (this technique has been applied to other type of materials and for other purposes [13]). Several experiments on microhardness were performed via instrumented indentation with recording the load versus penetration depth curves [14].

Investigations revealed that the properties of the epoxy and nanocomposites depend on aging factors. Because of this, the properties of samples tested over a period of 1-1.5 years after their

preparation (aging samples) as well as of the same samples after prolonged aging (2-3 years) at room temperature (aged samples) are described.

## 3. Experimental results and discussion

At first the data obtained on the aging (structurally unstable) samples will be described, and then the results of research of the rheological properties of the aged (structurally stable) samples will be presented.

*3.1. Structure of composites*. X-ray investigation revealed that the samples used have no crystalline component and are amorphous objects with quite large short-range order domains of 2.5-2.8 nm. This is indicated by the broad intensive haloes at small diffraction angles $2\theta$ = (6-7) deg. The X-ray diffraction patterns have no coherent scattering peaks that are characteristic of crystalline long-range order phases (Fig. 1).

The processed X-ray diffraction data are given in Table 1. It is seen that the additives to epoxy resin have an appreciable effect on the structural state of the matrix. The introduction of a block copolymer in the matrix (CE sample) suppresses the halo intensity almost by half (Fig. 1*a* and Table 1). It is possible that the observed result is due to a homogenization of the basic polymer. The addition of single- or multiwall carbon nanotubes into the matrix suppresses the integral intensity of the halo, reduces its width and shifts it towards smaller angles (Fig. 1*b,* Table 1).

There is little distinction between the diffraction patterns of three-component systems (samples CCM, CCS) and the epoxy resin+copolymer. The position of the halo maximum corresponds to the angles for the basic polymer matrix, but its intensity changes in different ways with the introduction of single- or multiwall nanotubes (see Table 1).

Table 1. Structural characteristics of epoxy resin-based composites

| Material | Angular position of halo, $2\theta$, deg. | Halo half-width, $\Delta$, deg. | Integral intensity of halo, I, imp/s | Size of short-range order domain, D, nm |
|---|---|---|---|---|
| ER | 6,72 | 3,11 | 15862 | 2.630 |
| CE | 7.02 | 2.83 | 7974 | 2.518 |
| ECM | 6.22 | 3.02 | 11114 | 2.842 |
| ECS | 6.45 | 3.08 | 12263 | 2.740 |
| CCM | 6.80 | 3.25 | 12633 | 2.598 |
| CCS | 6.84 | 2.88 | 6722 | 2.584 |

*Note:* ER = epoxy resin; CE = epoxy resin+copolymer; ECM = epoxy resin+multi-wall carbon nanotubes; ECS = epoxy resin+single-wall carbon nanotubes; CCM = epoxy resin+multi-wall carbon nanotubes+copolymer; CCS = epoxy resin+single-wall carbon nanotubes+copolymer.

The presence of CNTs in epoxy resin shows up not as individual diffraction but through their influence on the shape and the position of the matrix halo. The latter indicates, apparently, some effect of carbon nanotubes on the intermolecular interaction in the matrix. The absence of diffraction from the CNTs may be due to their low concentration in the samples.

*3.2. Microhardness at room temperature.* A large body of research shows that the experimentally measured hardness depends on the test load, especially at small loads (so called indentation size effect – ISE). With this in mind, the dependences of the impression diagonal length on load were plotted in the $d^2 - P$ coordinates (Fig. 2). This enabled us to estimate the microhardness from the straight line slopes, $H_{\mathrm{V}} = 1.854 \dfrac{\mathrm{d}P}{\mathrm{d}\left(d^2\right)}$ and exclude the noncontrollable influence of some factors responsible for the ISE. The obtained $H$V-values are within the region where $H$V is independent of the load $P$ and characterize the total resistance to indentation of the material and a deposited film on its surface.

The types of materials and their $H$V-values obtained by different techniques are given in Table 2. As the instrumented indentation data show, the samples are very soft at room temperature. Vacuum deposition of even a thin film of much harder Al ($H$V = 200 MPa at room tempera-

ture) increases the microhardness considerably. An In film deposited on the sample surface (it is ten times less hard than Al - $H_V$ = 20 MPa) had a much weaker effect on $H_V$.

Table 2. Microhardness $H_V$ of the epoxy resin and composites on its basis at room temperature (except the fresh cut measured at $T \leq 280$ K) obtained by various techniques

| Material | Microhardness $H_V$, MPa | | | | |
|---|---|---|---|---|---|
| | Surface condition of sample or indenter | | | | Instrumented indentation |
| | Fresh cut $T \leq 280$ K | Al film 40 nm | In film 10 nm | Ramsay lubrication | |
| ER | 1.87 | 2.72 | 2.34 | 1.79 | |
| CE | | 3.03 | 2.34 | | 2.2 |
| CCM | 2.41 | 3.4 | 2.48 | 2.04 | 2.2 |
| CCS | 5 | | | | |

The Ramsay lubrication grease on the indenter pyramid surface decreased the hardness values in comparison with the instrumented indentation data. This may be due to reduction of the friction between the pyramid surface and the material during indentation.

According to the instrumented indentation data the addition of CNT into epoxy resin had no effect on the microhardness value of composite. The result is in agreement with the statement that "generally, the in-plane tensile properties of a fiber/polymer composite are defined by the fiber properties, while the compression properties … are defined by the characteristics of matrix resin" [15]. Under indentation tests, hydrostatic compression is the most part of deformation. Low content of CNT in composites, their sparse distribution in the epoxy resin and the flexibility of nanotubes can also be responsible for the lack of the reinforcing effect at the action of a point load.

*3.3. The microhardness change at lower temperatures.* As the temperature was decreased, impressions started to appear on the sample surface – first those made by the diamond pyramid edges and then complete residual impressions. At room temperature, the depression from the penetration of the indenter pyramid into epoxy resin disappears when the indenter is moved off. That is, the deformation in the impression area is fully reversible. At the cooling of the sample, the re-

versible (elastic) part of the deformation under the indenter decreases and the irreversible (forced elastic) component increases. The emergence of the residual impressions indicates the onset of the glass transition. The change in the form of the impression is illustrated in Fig. 3.

In the DMA tests the temperature of the glass transition, $T_g$, of elastomers corresponds to the temperature of the peak of internal friction. The peak agrees with the onset of the rise in modulus [5]. In our measurements we can compare the evolution of impressions (or the behavior of microhardness) with the temperature dependence of modulus. These observations show that the microindentation method is an efficient tool of investigating structural transitions in polymers from the state close to the high elasticity to the glass structure.

The glass formation in the investigated materials began at $T \approx 280$ K. Then the temperature of the onset of the glass transition increased by about 10 K on repeated measurement on the same sample. This suggests instability of the structural properties of the samples.

The $H_V$ values calculated from the length of the residual impression diagonal cannot account adequately for the mechanical properties of the investigated composites, especially at the temperatures of the onset of the glass transition. There are two reasons for this inaccuracy. Firstly, because of a partial recovery, the diagonal of the residual impression can be shorter than the initial one in the loaded state. Secondly, it is proper to calculate microhardness from the true area of the indenter – material contact rather than from the area of the residual impression surface which is usually calculated as the squared diagonal of the residual impression divided by 1.854 for Vickers pyramid (see Eq. (1)). These areas can differ considerably for elastomers: the real contact area is normally smaller than the area calculated by the last procedure [16]. These two factors can partly counterbalance each other but the true magnitudes of microhardness are still a challenge calling for more special investigations [16]. Such problems are absent for glassy materials. Thus, the $H_V$ values measured at the temperatures at which composites are approaching the high-elastic state can provide only a qualitative description of the mechanical properties of materials. However, as

the temperature of indentation decreases, the data approximate to the true values for the lower temperature regimes.

The temperature dependences of microhardness for pure epoxy resin ER and the CCS composite are quite close (see Fig. 4).

*3.4. Instability of the micromechanical properties of the aging samples.* The temperature dependence of microhardness measured on the same CCS composite sample on different days is illustrated in Fig. 4. The first measurement on the CCS sample (curve 1) shows that a slight decrease in the temperature causes a fivefold increase in the microhardness. This strengthening is produced by the structural elastomer-glass transition that develops gradually on cooling. The glass transition temperature is obviously below 262 K. The repeated measurement on the same CCS sample a week later (curve 2) revealed significant changes in the temperature dependence of microhardness: impressions started to appear at a higher temperature, the microhardness increased at $T > 275$ K and the temperature of glass formation decreased.

The unstable properties were characteristic of all fresh samples of the investigated composites. The instabilities may be caused by natural ageing at room temperature and by repeated cooling-heating cycles. However, no thorough investigation of this problem has been performed so far. Hereafter, we studied more stable samples aged at room temperature under ambient conditions during more than two years. This allowed a series of experiments to be made where the reproducibility of the results of measurements is of importance. Elastomer CE was studied in sufficient detail, however all features of the thermomecanical properties of this elastomer was reproduced in studies of the rest of materials listed in Table 1 too.

*3.5. Measurement of the glass transition of the elastomer by microindentation.* It was shown in Section 3.3 that the microhardness of the studied materials sharply increases on cooling below 270 K. This indicates the onset of the high elasticity-glass transition of elastomers. To study in more detail this transition, we measured the temperature dependence of microhardness of elastomer CE over a sufficiently wide interval from 300 K to 230 K on cooling as well as heating with

a small temperature step (about 1 K) (Fig. 5). As seen in the figure, the microhardness changes dramatically within a narrow temperature interval of 265-240 K and continues to change weakly beyond this range. General change of microhardness under cooling from 287 K to 230 K was 25-fold – from 10 MPa to 250 MPa. As also seen in Fig. 5, this effect is reversible on a qualitative level: microhardness decreased equally drastically and the ration of $H_V$ values on the edges of the temperature interval studied $\frac{H_V(230\ K)}{H_V(295\ K)}$ was even more marked (of order 60).

The values of microhardness have a rather significant statistical scatter probably related to the inhomogeneity of the sample surface on a length of order of the linear size of impression. The points in Fig. 5 are the result of the averaging of measurements in the interval of $\Delta T \approx$ 1-2 K.

The dependence $H_V(T)$ in Fig. 5 reflects the high elastic state to glass transition of the polymer. The temperature dependence of microhardness can be approximated by a step-like (sigmoidal) curve adequately. The coordinate of the midpoint of the step in the $H_V(T)$ curve obtained at the cooling of the sample was considered as the glass-transition temperature $T_g'$ by convention. A similar dependence of $H_V(T)$ is observed at heating of sample too, that is, this transition may be considered as a reversible one at a first approximation: the coordinate of the midpoint of the step in the $H_V(T)$ dependence can be considered as a softening temperature $T_g''$. At the slow temperature change with the rate of $\dot{T} \leq$ 0.5 K/s the temperatures of glass-transition and softening coincided: $T_g' = T_g'' = T_g$. But at heating in the vicinity of the high elastic state the $H_V(T)$ dependence does not coincide with the one obtained at cooling (see the insert on Fig. 5).

To reveal the high elastic state-glass transition of a polymer using mechanical tests, the value of the macroscopic deformation of creep evolving at a constant stress over a fixed time (thermomechanical curve) [9,10] or the reaction of the sample on cyclic loading (internal friction method) are usually employed. At cycling tests, the maximum of the mechanical losses and/or the step on the temperature dependence of the dynamic elastic modulus correspond to the glass-transition temperature. The dependence of the Young's module of the cured composites based on

the epoxy resin [5,17,18] (including those with single-wall [5] or multi-wall [18] CNT's) are similar in aspect to the $H_V(T)$ curve on Fig. 5. The correspondence allows to assume the existence of a direct relation between the microhardness and the Young's modulus $H_V = \beta E$.

*3.6. The influence of thermocycling and the displacement of the $H_V(T)$ curve at the change of loading duration.* Repeated cooling-heating of the same specimen showed that the thermocycling had no effect on the general form of the temperature dependence of microhardness. But some quantitative changes were observed from cycle to cycle, the glass-transition temperature $T_g$ experienced nonsystematic oscillations in part. The values of the glass-transition temperature and the softening temperature coincided practically within the first cycle, if the rate of the temperature change was sufficiently small. The scatter of the $T_g$ values in different cycles may be related to the disruption of the equilibrium structure of material after deformation and/or cooling at the foregoing cycles. The dissimilar values of microhardness at the cooling and subsequent heating in the temperature range $T > T_g$ (see the insert on Fig. 5) indicate that the inner structure of sample was changed at cooling.

The observation described above demanded some caution at the investigation of the effect of the loading duration $\Delta t$ on the shift of the sigmoidal curve $H_V(T)$. To get the $T_g(\Delta t)$ dependence all measurements were performed in one cooling-heating cycle. The sequence of measurements was as follows: at a fixed temperature a set of impressions were made at some selected loading duration $\Delta t$ = 10, 30, and 60 s. Once the diagonal lengths were measured, the temperature was decreased and the indentation process was repeated. In this way, the temperature dependence of microhardness, $H_V(T)$, was obtained at the different values of $\Delta t$ in the temperature interval from 300 K to 230 K. The results of measurements for one of the specimens of the CE elastomer are shown in Fig. 6. As it can be seen from the figure, the glass transition temperature, $T_g$, is monotonically decreasing with the loading duration, $\Delta t$, increasing.

The $T_g(\Delta t)$ dependence suggests that the $T_g$ must be considered as a kinetic transition and not as thermodynamic one. The temperature dependence of microhardness, $H_V$(T), and the load-

ing-duration dependence of the glass transition temperature, $T_g(\Delta t)$, are evidently determined by the character of the temperature-dependent motion of the molecular segments responsible for the glass transition effect.

**4. Rheological properties of the studied materials**

In this section, a phenomenological analysis of the thermomechanical experimental results of the elastomer and its nanocomposites obtained by microindentation is presented. The results are discussed in the terms of the rheological model of the standard linear solid which is frequently used for the description of viscoelastic behavior of polymeric materials at different types of mechanical tests. They are also analyzed on the basis of the concept of the thermally activated motion of molecular segments.

*4.1. Determining rheological equations.* In Section 3.1 it was shown that both the nanocomposites based on epoxy resin and the pure epoxy resin under study are isotropic materials. At sufficiently low temperature (far lower than the glass transition temperature $T_g$) they can be considered as isotropic elastic solids with mechanical properties which in linear approximation (small deformations) are characterized by two independent components of the elastic moduli tensor: for example, the Young's modulus $E$ and the Poisson's ratio $\nu$. At the tension of elastic bars the Hooke's law is satisfied, whereby instantaneous local values of relative strains of the axial tension $\varepsilon_l(x,t)$ and the lateral (transverse) contraction $\varepsilon_t(x,t)$ ($x$ is the coordinate along the bar axes) are connected with the deforming stress $\sigma(x,t)$ at the cross section of the bars by the following relations:

$$\sigma(x,t) = E\varepsilon_l(x,\, t), \tag{2}$$

$$\varepsilon_t(x,\, t) = -\,\nu\varepsilon_l(x,\, t). \tag{3}$$

Elastomers' Poisson's ratio (above and at the glass transition region) has a value of $\nu \approx 0.5$ and practically does not depend on temperature. However, the relation between $\sigma$ and $\varepsilon_l$ for visco-

elastic elastomers is determined by more complicated equations than the Hook's law (2). This equation must take into account both nonsynchronous changes of strain $\varepsilon_l(x,t)$ and stress $\sigma(x,t)$ (the aftereffect) and internal friction (mechanical energy dissipation).

The standard linear solid is generally considered [19] as a sufficiently universal rheological model of an isotropic elastomer. In this case the equation determining the relation between $\varepsilon_l$ and $\sigma$ contains three parameters: two of them, $E_1$ and $E_2$, have the dimensionality of elastic modulus, while the third parameter plays the role of viscosity, $\eta$ with a corresponding relaxation time $\tau = \eta/E_2$. The creep of this elastomer at macromechanical tests [20] or under indentation [21] is described by a simple exponential law with a single relaxation time. For a standard linear solid the main rheological equation which substitutes the Hook's law (2) is conveniently represented as follows:

$$\sigma + \frac{E_\infty}{E_0}\tau\dot{\sigma} = E_\infty(\varepsilon_l + \tau\dot{\varepsilon}_l), \tag{4}$$

where

$$\tau = \eta\frac{E_0 - E_\infty}{E_0 E_\infty}.$$

Here the derivatives of the corresponding values with respect to time are indicated by the symbols $\dot{\sigma}$ and $\dot{\varepsilon}_l$; the time relaxation $\tau$, the nonrelaxed $E_0$ and relaxed $E_\infty$ Young's moduli were chosen as the model parameters.

*4.2. Indentation creep of an elastomer.* We will use the results of theoretical studies [21-23] where the Hertz classical contact problem for ideal elastic materials was solved in the case of rigid indenter penetration in a viscoelastic material. In particular, in [21], the microcreep of a viscoelastic material under the action of a conical indenter is described. The rheological properties of the material are specified by the relations (2), (3) and (4).

Analyzing the indentation creep of the viscoelastic material, two specific properties of this process must be taken into account. Firstly, in the indentation region, a nonuniform strained state is realized and a complex mixture of hydrostatic compression, tension, and shear is generated. Thus the indentation microcreep depends not only on the parameters of the equation (4), $E_0$, $E_\infty$,

and $\tau$, but on the Poisson's ratio $\nu$ as well. Secondly, at a constant load $P$ on indenter, the strain is accompanied by the progressive decrease of the stress in the contact area because of the increase of the indenter-material interface. The correct account of these features when solving the contact problem [21] leads to the following dependence of the depth of penetration $h$ of a rigid conical indenter on time in material with the rheological properties (3) and (4):

$$h^2(t,\tau) = P\frac{(1-\nu^2)\pi\cot\vartheta}{2E^*(\tau^*;t)}. \qquad (5)$$

Here $P$ is a steady applied load, $\vartheta$ is an apex angle of the indenter, and $E^*(\tau^*;t)$ is an effective Young's modulus of material which is determined as follows:

$$\frac{1}{E^*} = \frac{1}{E_0} + \frac{E_0-E_\infty}{E_0E_\infty}\left(1-e^{-\frac{t}{\tau^*}}\right), \qquad \tau^* = (1-\nu^2)\tau. \qquad (6)$$

Notice that the expression (5) agrees formally with the solution of the classical Hertz problem if $E^*$ in it is substituted by the Young's modulus of an ideal elastic solid.

For the Vickers pyramid, $\vartheta = 68^0$ and the impression diagonal $d = 7h$, hence the time dependence of $d = d(\tau^*;t)$ is described by the formula:

$$d^2 = P\frac{31.1\,(1-\nu^2)}{E^*(\tau^*;t)}. \qquad (7)$$

At the microhardness measurement, the indentation duration has a fixed value $t = \Delta t$. By substituting (7) in (1), we obtain the formula for $H_V(\tau^*;\Delta t)$:

$$H_V = \frac{0.06}{1-\nu^2}E^*(\tau^*;\Delta t). \qquad (8)$$

*4.3. The viscosity and the glass transition of an elastomer as a consequence of the thermally activated motion of molecules.* The formulae (6)-(8) describe the duration dependence of indentation creep deformation and microhardness of an elastomer. They are a consequence of accounting, in the rheological equation (4), of the aftereffects and the viscosity, which are characterized by the parameter $\tau$. However, for the analytical description of the influence of the temperature $T$

and the glass transition on the microhardness, it is necessary to point an explicit form of the temperature dependence of all parameters of the considered rheological model.

The experimental results listed in Section 3 allow a consistent quantitative description of them on the basis of the rheological model (3)-(4) if it is supplemented by two assumptions:

- elastic moduli $E_0$, $E_\infty$ and Poisson's ratio, $\nu$ have no significant temperature dependence within the temperature range of interest, near and higher of the glass transition temperature $T_g$;
- the parameter $\tau$ as a characteristic of the deformation viscosity of material has an exponential temperature dependence.

When describing the properties of elastomers at the molecular level, these assumptions correspond to the notion that both the relaxation properties of elastomer and its glass transition are caused by the thermally activated motion of molecular segments [9,10]. This means that the relaxation time $\tau$ must have a characteristic dependence on temperature, corresponding to the Arrhenius law for the rate of behavior of thermally activated processes:

$$\tau(T) = \tau_0 exp\left(\frac{U}{kT}\right). \tag{9}$$

It is generally assumed that the period of attempts $\tau_0$ and the activation energy $U$ do not depend significantly on temperature, although in some cases a quantitative description of the experiment cannot be obtained without abandoning this assumption [10,12].

The joint use of the formulae (6) - (9) allows to obtain the theoretical description of the thermomechanical properties of elastomers investigated by microindentation (see Section 3), as well as to check the adequacy of the rheological model discussed with the features observed in the experiments, obtaining the empirical estimates of the model parameters $E_0$, $E_\infty$, $\tau_0$, and $U$.

We will concentrate to two main features of the observed behaviour: the sharp rise of microhardness within narrow temperature interval at lowering temperature which is due to the glass

transition and the asymptotically athermal behavior of microhardness at sufficiently high and low temperatures.

Since the relaxation time $\tau^*(T) = (1 - \nu^2)\tau(T)$ has a monotonic exponentially sharp temperature dependence, it follows from the formulae ((6)-(9) that the temperature dependence of microhardness $H_V(T;\Delta t) \equiv H_V[\tau(T);\Delta t]$ has the form of a step-like curve which was registered in experiments (Fig. 5 and Fig. 6). The glass transition temperature $T_g$ was determined by us as a coordinate of the middle-point of the step on Fig. 5; the relaxation time corresponding to this temperature is denoted as $\tau_g = \tau(T_g)$. It is can be deduced from the formulae (6)-(9) that in the limiting cases $\tau_g >> \Delta t$ ($T << T_g$ – the glass state) and $\tau_g << \Delta t$ ($T >> T_g$ – the high elastic state) the following asymptotical relations are satisfied:

$$H_V(T;\Delta t) = \begin{cases} H_V^{(max)} = \frac{0.06}{1-\nu^2} E_0, \quad T \ll T_g; \\ \\ H_V^{(min)} = \frac{0.06}{1-\nu^2} E_\infty, \quad T \gg T_g. \end{cases} \tag{10}$$

The approaching of $H_V$ to the limiting values which are temperature independent is clearly seen in Fig. 5 and Fig. 6. The results of measurements bring to the relation $H_V^{(\min)} \ll H_V^{(max)}$ between the limiting values of microhardness; consequently, the elastic moduli of the rheological model of the elastomer studied must satisfy the inequality $E_\infty << E_0$. The results of the measurements of microhardness shown in Fig.5 and Fig. 6 and the formula (10) allow us to obtain the empirical estimates of the parameters $E_0$ and $E_\infty$. However, it has to be noted that the wide statistical scatter of the experimental data and the temperature hysteresis of microhardness allow only an order of magnitude of values:

$$\bar{E}_0 \approx 2.5 \cdot 10^9 \text{ Pa}, \quad \bar{E}_\infty \approx 1 \cdot 10^8 \text{ Pa}. \tag{11}$$

Furthermore, the formulae (6)-(9) allow us to establish the dependence of the glass transition temperature $T_g(\Delta t)$ on the loading duration at the microhardness measurements. This dependence is implicitly determined by the relation:

$$H_V(T_g; \Delta t) = \frac{1}{2}\left(H_V^{(max)} - H_V^{(\min)}\right).$$

Taking into account that for the studied elastomer $E_\infty << E_0$ and that for a temperature range close to the glass transition temperature $\Delta t << (1 - \nu^2)\tau(T_g)$, in the basic small-parameter approximation, we obtain the relation:

$$\frac{1}{T_g} = \frac{k}{U} ln\left[\frac{E_0 \Delta t}{(1-\nu^2)\tau_0 E_\infty}\right]. \quad (12)$$

The formula describes a logarithmically weak decrease of $T_g$ with increasing $\Delta t$ that is in a qualitative agreement with the experimental results shown on Fig. 6.

An empiric estimation of the activation energy $U$ can be obtained using the analysis of the temperature dependence of $H_V(T;\Delta t)$ at one value for $\Delta t$ but over a sufficiently wide temperature range in vicinity of $T_g$ (Fig. 5 and Fig. 6). By the simple rearrangements of the formulae (6), (8) and (10) the relation can be obtained which allows to find the temperature dependence of the relaxation time $\tau(T)$ using the temperature dependence of microhardness $H_V(T)$ at a given value of the indentation duration $\Delta t$:

$$\tau(T) = \frac{\Delta t}{1-\nu^2}\left\{ln\left[\frac{H_V(T)}{H_V^{(max)}} \cdot \frac{H_V^{(max)} - H_V^{(min)}}{H_V(T) - H_V^{(min)}}\right]\right\}^{-1}. \quad (13)$$

Fig. 7 shows the temperature dependence of the relaxation time $\tau(T)$ obtained by substitution of the $H_V(T)$ values from Fig. 6 at $\Delta t = 10$ s and $\nu = 0.5$ into the right part of the formula (13). One can see from the figure that this dependence has an exponentially sharp character and allows the analytical approximation (9) of the parameters:

$$\tau_0 = 10^{-12} \text{ s}, \; U = 0.75 \text{ eV}. \quad (14)$$

Notice that this result and the estimations obtained for $\tau_0$ and $U$ are the same also for analyses of the experimental values of $H_V(T)$ gained for the other values of the indentation duration (with an accuracy of the statistical scatter of the results of the measurements). The magnitudes of $\tau_0$ and $U$

are typical of the $\alpha$-process at the transition of polymer from hard to high elastic state where conformation dynamics (segmental mobility) of polymer molecules starts [12, 14].

The above-performed analysis of the experimental data allows concluding that the relaxation properties and the glass transition of these elastomers are determined by the thermally activated molecular processes with the estimated activation parameters (14). In accordance with the classification developed in physics of polymers [9,10] this process is associated with the so called α-relaxation, resulting from the thermal motion of the comparatively small (nanometer) segments of macromolecular chains comprising the elastomer.

## 5. Conclusion

In this paper, we have used microindentation to study the thermomechanical and relaxation properties of a number of polymer compositions based on epoxy resin: pure epoxy resin (ER), epoxy resin+block-copolymer (CE), CE+single-wall or multi-wall carbon nanotubes (CNT). Microindentation of these materials in the temperature range 300-230 K showed that at room temperature all of them are in a high-elastic state and transform to a glass state upon the cooling in the interval 270-250 K. At a fairly small concentration of CNTs in the epoxy resin, microindentation does not permit to reveal their strengthening effect on the polymer. However, the method allows the study of the stability of the structural states of polymers with time and at various thermocycles. Moreover, the experimental results obtained and their analysis suggest that microindentation is an effective method of relaxation spectroscopy of polymers: firstly, it permits a reliable measurement of the structural relaxation processes at the state near the high-elastic state and monitoring the glass transition process; secondly, the analysis of the experimental data on a basis of the existing theory allows one to obtain empirical estimations of both polymer nonrelaxed and relaxed Young's moduli ($\bar{E}_0 \approx 2.5 \cdot 10^9$ Pa, $\bar{E}_\infty \approx 1 \cdot 10^8$ Pa) in addition to the molecular-kinetic parameters of the structural relaxation ($\tau_0 = 10^{-12}$ s, $U = 0.75$ eV).

**Acknowledgement** The Kharkiv authors thank Dr. A.A. Solodovnik for the vacuum deposition of metal films on the specimen surfaces of elastomers, and Professor Yu.V. Milman for

help with the instrumented microhardness measurement of elastomers. Financial support from National Academy of Sciences of Ukraine (project 0118U100347) is gratefully acknowledged.

**References**

1. M.-F. Yu, B.S. Files, S. Arepalli, R.S. Ruoff, *Phys. Rev. Lett.* **84**, 5552 (2000).
2. L.C. Qin, X. Zhao, K. Hirahara, Y. Miyamoto, Y. Ando, S. Iijima, *Nature* **408**, 50 (2000).
3. A.V. Eletskii, *Physics-Uspekhi* **45** 369–402 (2002).
4. Kin-Tak Lau, San-Qiang Shi, Li-Min Zhou, Hui-Ming Cheng, *J. Comp. Mater.* **37**, 365 (2003).
5. Yu-Hsuan Liao, Oliver Marietta-Tondin, Zhiyong Liang, Chuck Zhang, Ben Wang, *Mater. Sci. Eng.* **A 385**, 175 (2004).
6. Xiaodong Li, Hongsheng, Wally A. Scrivens, Dongling Fei, Xiaoyou Xu, Michael A. Sutton, Anthony P. Reynolds, Michael L. Myrik, *Nanotechnology* **15**, 1416 (2004).
7. Qianqian Li, Michael Zaiser, Vasileios Koutsos, *Phys. Stat. Sol.* (a) **201**, R89 (2004)
8. Qianqian Li, Michael Zaiser, Jane R Blackford, Chris Jeffree, Yehong He, Vasileios Koutsos Materials Letters 125, 116-119, 2014
9. V.E.Gul, V.N.Kuleznev. Structura i mehanicheskije svoistva polimerov. - Moskva, Vysshaja Shkola, 1972.
10. G.M. Bartenev, Yu.V. Zelenev. Fizika i mechanika polimerov. - Moskva, Vysshaja Shkola, 1983.
11. Kevin P. Menard. Dynamic Mechanical Analysis. A Practical Introduction. CRC Press, 2008.
12. A.I. Slutsker, Yu.I. Polikarpov, K.V. Vasil'eva, *Phys. Sol. State* **44**, 1604 (2002).
13. Yu.S.Bojarskaja D.Z.Grabko, M.S.Kats. Fizika protsessov mikroindentirovanija. – Kishnev,Shtiintsa, 1986.
14. B.A. Galanov, O..N. Grigogev, Yu.V. Milman, *Problemy prochnosti* № 11, 93 (1983).
15. Yuanxin Zhou, Farhana Pervin, Lance Lewis, Shaik Jeelani, *Mater. Sci. Eng.* A **452-453**, 657 (2006).
16. Yung Yee Lim, M. Munawar Chaudhri, *Mech. Mater.* **38**, 1213 (2006).

17. Y. Zhou, F. Pervin, l. Lewis, Sh. Jeelani, *Mater. Sci. Eng.* A **452-453**, 657 (2006).

18. Sh. Deng, M. Hou, L. Ye, *Polymer Testing* **26**, 803 (2007).

19. M. Reiner. Rheology. – Berlin-Göttingen-Heidelberd, Springer-Verlag 1958.

20. T. Alfrey. Mechanical behavior of high polymers. Interscience, New York, 1948.

21. A.C. Fischer-Cripps, *Mater. Sci. Eng.* A **385**, 74 (2004).

22. E.H. Lee, J.R.M. Radok, *Trans.* ASME, *J. Appl. Mech.* **27**, 438 (1960).

23. I.N. Sneddon, *Int. J. Eng. Sci.* **3**, 47 (1965).

L.S. Fomenko S.V. Lubenets, V.D. Natsik , A.I. Prokhvatilov, N.N. Galtsov,
Q.Q. Li, V. Koutsos

За допомогою мікротвердоміра з низькотемпературним пристроєм вивчені механічні властивості епоксидної смоли і нанокомпозитів  епоксидна смола-вуглецеві нанотрубки. Аналіз дифракції рентгенівських променів показав, що всі зразки не містять кристалічних складових і є аморфними з доменами близького порядку. Оцінена мікротвердість всіх зразків в інтервалі температур 230-300 К. Вимірювання показали, що при кімнатній температурі ці матеріали мають властивості еластомерів (тобто знаходяться у високоеластичному стані), а в інтервалі температур 250-270 К має місце перехід у стан скла. Аналіз температурної залежності мікротвердості показав, що термомеханічні і релаксаційні властивості вивчених матеріалів узгоджуються з реологічною моделлю стандартного лінійного твердого тіла, для якого час релаксації (або в'язкість) експоненціально залежить від температури згідно з рівнянням Арреніуса для швидкості термоактивованого процесу. Одержано емпіричні оцінки нерелаксованого і релаксованого модулів Юнга, а також енергії активації ($U$ = 0.75 еВ) і періоду спроб ($\tau_0 = 10^{-12}$ с) молекулярного процесу, який визначає релаксаційні властивості і перехід матеріалів у стан скла. Додавання вуглецевих нанотрубок в епоксидну смолу не вплинуло на мікромеханічні характеристики. Показано, що традиційний метод мікроіндентування – це ефективний спосіб вивчення термомеханічних властивостей еластомерів поблизу та нижче температури переходу у стан скла.

L.S. Fomenko S.V. Lubenets, V.D. Natsik , A.I. Prokhvatilov, N.N. Galtsov,
Q.Q. Li, V. Koutsos

С помощью микротвердомера с низкотемпературной приставкой изучены механические свойства эпоксидной смолы и нанокомпозитов эпоксидная смола-углеродные нанотрубки. Анализ дифракции рентгеновских лучей показал, что все образцы не содержали кристаллических составляющих и являлись аморфными с доменами ближнего порядка. Оценена микротвердость всех образцов в интервале температур 230-300 К. Измерения показали, что при комнатной температуре эти материалы являются эластомерами (т. е. находятся в высокоэластическом состоянии), а в интервале температур 250-270 К имеет место переход в состояние стекла. Анализ температурной зависимости микротвердости показал, что термомеханические и релаксационные свойства изученных материалов согласуются с реологической моделью стандартного линейного твердого тела, для которого время релаксации (или вязкость) экспоненциально зависит от температуры в соответствии с уравнением Аррениуса для скорости термоактивированного процесса. Получены эмпирические оценки нерелаксированного и релаксированного модулей Юнга, а также энергии активации ($U$ = 0.75 эВ) и периода попыток ($\tau_0 = 10^{-12}$ с) молекулярного процесса, определяющего релаксационные свойства и переход материалов в состояние стекла. Добавление углеродных нанотрубок в эпоксидную смолу не повлияло на микромеханические характеристики. Показано, что традиционный метод микроиндентирования является эффективным способом для изучения термомеханических свойств эластомеров вблизи и ниже температуры перехода в состояние стекла.

Подписи под рисунки

Fig. 1. Small-angle scattering from ER and CE (a) and ER and ECM (b) samples.

Fig. 2. Influence of the load indentation $P$ on the diagonal length of the impression $d$ for ER, CE and CCM. $T$ = 290 K, the loading duration $\Delta t$ = 10 s. The measurements were performed on the specimens with the Al film of the thickness about 40 nm.

Fig. 3. Changes in the form of impressions at lowering temperature, (a) - 280 K, (b) – 275 K, (c) – 271 K, (d) - 265 K. Load $P$ = 0.05 N, loading duration $t$ = 10 s.

Fig. 4. The temperature dependence of microhardness of the epoxy resin – single-wall carbon nanotubes+copolymer composite (CCS) (curves 1, 2; curve 2 was obtained a week later) and pure epoxy resin (ER) (curve 3). $P$ = 0.01 N, $t$ = 10 s.

Fig. 5. The temperature dependence of microhardness $H_V(T)$ of elastomer CE obtained on cooling (1) and heating (2) at $P$ = 0.05 N and $\Delta t$ = 10 s. In the insert – temperature hysteresis of the dependence close to the high-elastic region.

Fig. 6. The temperature dependence of microhardness of elastomer CE at $P$ = 0.05 N and three values of the indentation duration $\Delta t$ = 10 s (1), 30 s (2) и 60 s (3).

Fig. 7. The temperature dependence of the relaxation time $\tau(T)$: the points indicate the values obtained by the substitution in the formula (14) the $H_V$ values from Fig. 6 at $\Delta t$ = 10 s; the solid line represents equation (9) using $\tau_0 = 10^{-12}$ s and $U$ = 0.75 eV (8720 K in the temperature units).

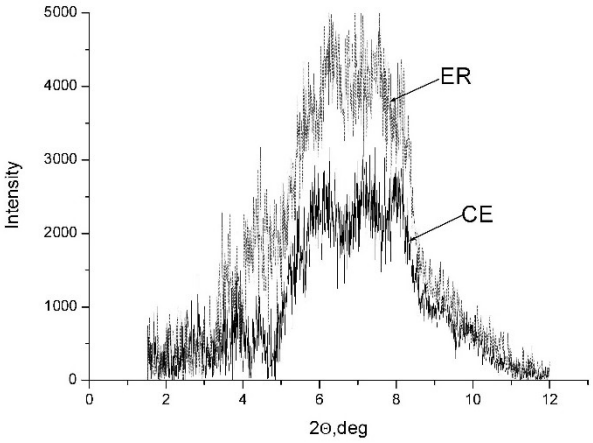


a)

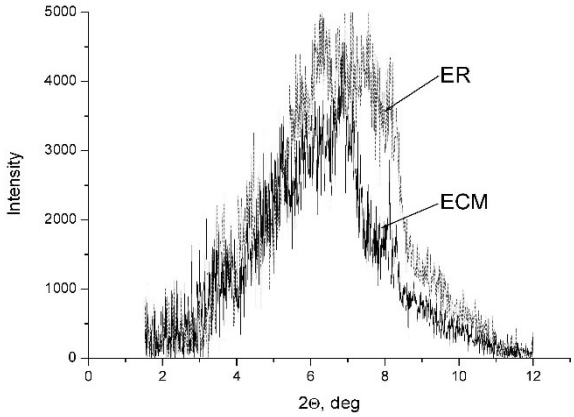


b)

Fig. 1. Small-angle scattering from ER and CE (a) and ER and ECM (b) samples.

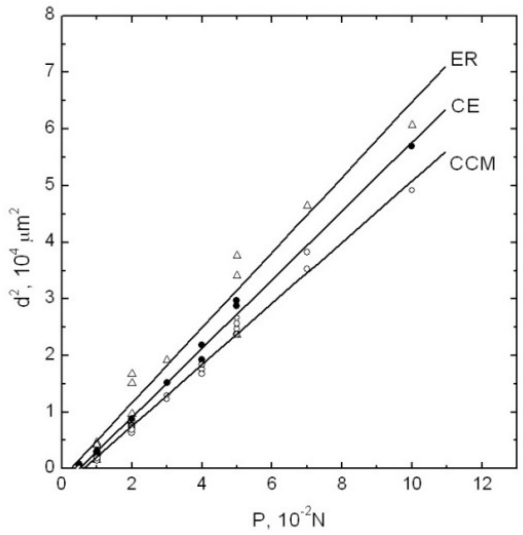


Fig. 2. Influence of the load indentation $P$ on the diagonal length of the impression $d$ for ER, CE and CCM. $T$ = 290 K, the loading duration $\Delta t$ = 10 s. The measurements were performed on the specimens with the Al film of the thickness about 40 nm.

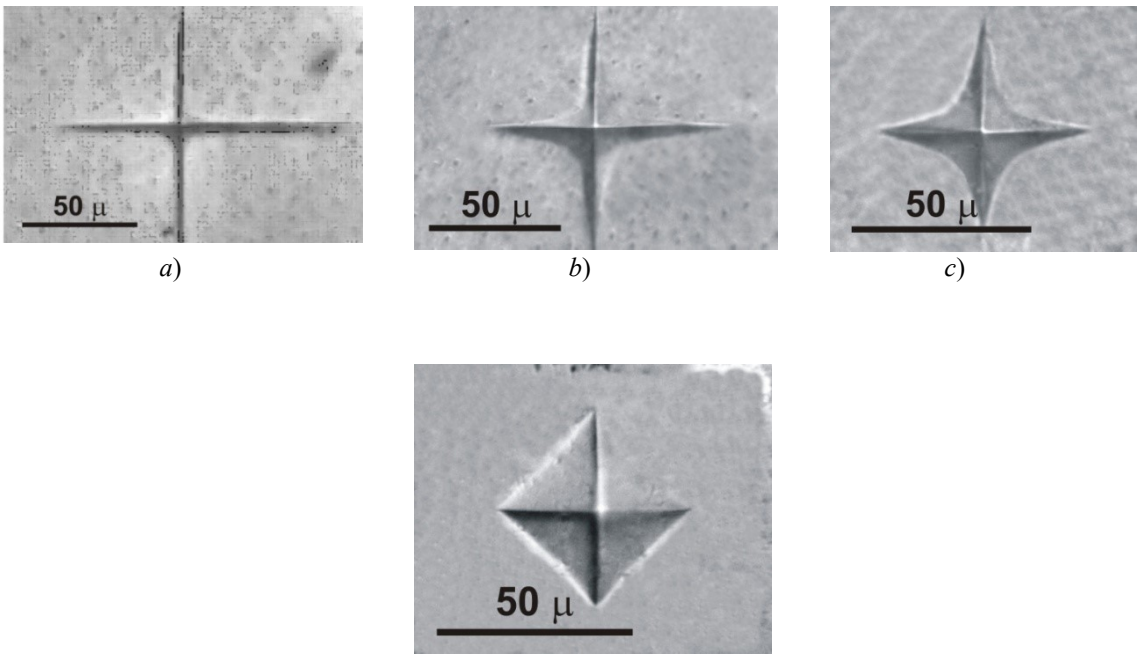


*a*) *b*) *c*)

*d*)

Fig. 3. Changes in the form of impressions at lowering temperature, (a) - 280 K, (b) – 275 K, (c) – 271 K, (d) - 265 K. Load $P$ = 0.05 N, loading duration $t$ = 10 s.

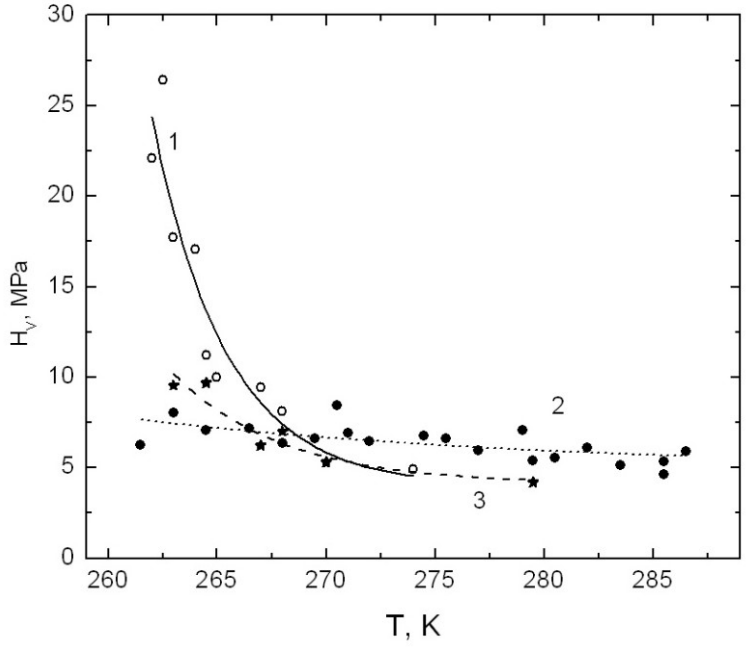


Fig. 4. The temperature dependence of microhardness of the epoxy resin – single-wall carbon nanotubes+copolymer composite (CCS) (curves 1, 2; curve 2 was obtained a week later) and pure epoxy resin (ER) (curve 3). $P$ = 0.01 N, $t$ = 10 s.

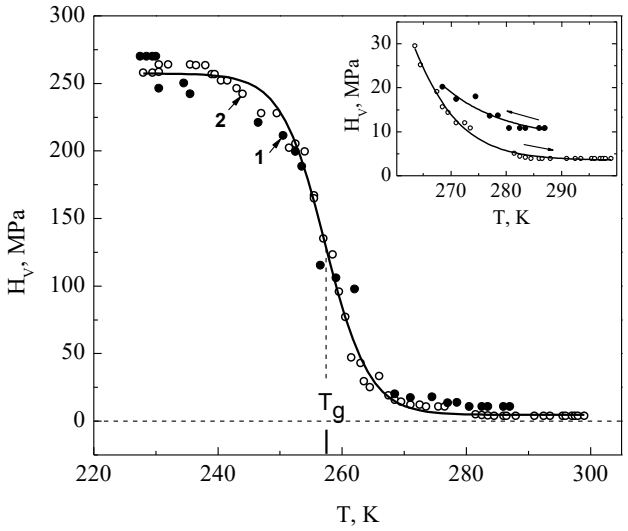


Fig. 5. The temperature dependence of microhardness $H_V(T)$ of elastomer CE obtained on cooling (1) and heating (2) at $P$ = 0.05 N and $\Delta t$ = 10 s. In the insert – temperature hysteresis of the dependence close to the high-elastic region.

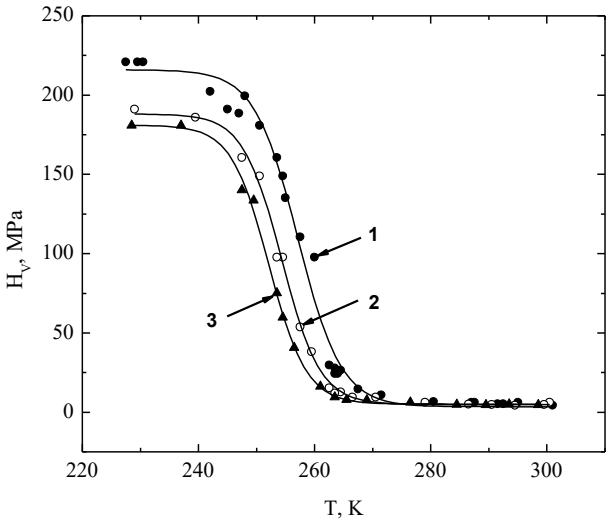


Fig. 6. The temperature dependence of microhardness of elastomer CE at $P$ = 0.05 N and three values of the indentation duration $\Delta t$ = 10 s (1), 30 s (2) и 60 s (3).

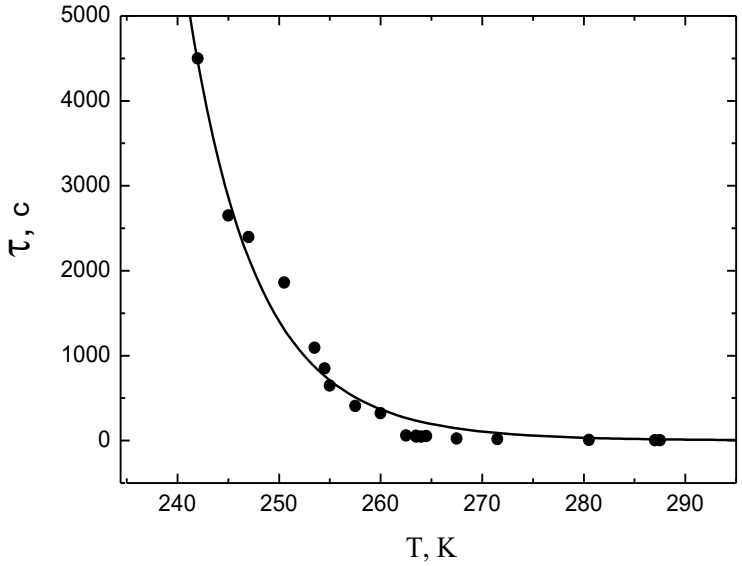


Fig. 7. The temperature dependence of the relaxation time $\tau(T)$: the points indicate the values obtained by the substitution in the formula (14) the $H_V$ values from Fig. 6 at $\Delta t$ = 10 s; the solid line represents equation (9) using $\tau_0 = 10^{-12}$ s and $U$ = 0.75 eV (8720 K in the temperature units).